AMERICAN JOURNAL OF PHYSIOLOGY
REGULATORY, INTEGRATIVE AND COMPARATIVE PHYSIOLOGY

Am J Physiol Regul Integr Comp Physiol 321: R951–R959, 2021.
First published October 27, 2021; doi:10.1152/ajpregu.00306.2020

RESEARCH ARTICLE

Translational Physiology

Activation of brain-heart axis during REM sleep: a trigger for dreaming

Mimma Nardelli,[1,2] Vincenzo Catrambone,[1,2] Giulia Grandi,[3] Tommaso Banfi,[3] Rosa Maria Bruno,[5] Enzo Pasquale Scilingo,[1,2] Ugo Faraguna,[3,4] and Gaetano Valenza[1,2]

[1]*Bioengineering and Robotics Research Centre E. Piaggio, University of Pisa, Pisa, Italy;* [2]*Department of Information Engineering, University of Pisa, Pisa, Italy;* [3]*Department of Translational Research and of New Surgical and Medical Technologies, University of Pisa, Pisa, Italy;* [4]*Department of Developmental Neuroscience, IRCCS Fondazione Stella Maris, Pisa, Italy; and* [5]*INSERM U970 Team 7, Paris Cardiovascular Research Centre—PARCC, University Paris Descartes, Sorbonne Paris Cité, Paris, France*

Abstract

Dreams may be recalled after awakening from sleep following a defined electroencephalographic pattern that involves local decreases in low-frequency activity in the posterior cortical regions. Although a dreaming experience implies bodily changes at many organ, system, and timescale levels, the entity and causal role of such peripheral changes in a conscious dream experience are unknown. We performed a comprehensive, causal, multivariate analysis of physiological signals acquired during rapid eye movement (REM) sleep at night, including high-density electroencephalography and peripheral dynamics including electrocardiography and blood pressure. In this preliminary study, we investigated multiple recalls and nonrecalls of dream experiences using data from nine healthy volunteers. The aim was not only to investigate the changes in central and autonomic dynamics associated with dream recalls and nonrecalls, but also to characterize the central-peripheral dynamical and (causal) directional interactions, and the temporal relations of the related arousals upon awakening. We uncovered a brain-body network that drives a conscious dreaming experience that acts with specific interaction and time delays. Such a network is sustained by the blood pressure dynamics and the increasing functional information transfer from the neural heartbeat regulation to the brain. We conclude that bodily changes play a crucial and causative role in a conscious dream experience during REM sleep.

autonomic nervous system; brain-heart interaction; dreams; electroencephalography; rapid eye movement

INTRODUCTION

Sleep is a fundamental aspect of life that influences the health of individuals and involves a large number of physiological processes. The interaction occurring between the central nervous system (CNS) and sleep has been explored over recent years, but the neural pathways coupling these CNS correlates and the autonomic nervous system (ANS) changes are still putative (1–3). In this regard, findings of previous studies highlight changes in cardiac vagal modulation according to CNS-defined sleep stages, spontaneous arousal in both autonomic signals and CNS- defined events, and linear and nonlinear time relationships between cortical and cardiovascular time series (1).

A limited number of studies focus on dreams mainly because of the difficulty in conducting experiments. Although recent findings have convincingly demonstrated that dream recall is a trustable research tool (4), such a paradigm also foresees the administration of ad hoc questionnaires after the subject's awakening.

One of main features of sleep is the weakening of consciousness. Dreams demonstrate that human physiological mechanisms alone can generate complex conscious experiences without any exchange with the environment. From waking through nonrapid eye movement (NREM) sleep stages, thoughts decrease gradually; however, the likelihood of dream recall increases strongly across these stages, reaching a peak in rapid eye movement (REM) sleep (5, 6). First attempts have been made to characterize dreaming physiology since the discovery of REM stage in 1953 (7) and, subsequently, its correlation with dreams (8, 9). In those pioneer studies, the occurrence of dreams was associated with high-frequency electroencephalography (EEG) activation during REM sleep (10). However, subsequent studies demonstrated the occurrence of dreaming experience during the NREM stages too, thereby changing the common understanding of conscious experience during sleep (6, 11). Recently, Siclari et al. (11) investigated the correlates of dream recall using high-density EEG. These authors revealed that, in both NREM

Correspondence: M. Nardelli (mimma.nardelli@unipi.it).
Submitted 28 October 2020 / Revised 13 October 2021 / Accepted 15 October 2021

and REM stages, dream experience recall was associated with a local decrease in low-frequency activity in the parieto-occipital region and with a concurrent increase in high-frequency activity in the frontal and temporal regions during REM sleep. In this study, we used the index proposed in the study by Siclari et al. (11) to describe brain activity changes during sleep (see *Processing of EEG signals* section below).

Physiological metrics extracted from heart rate variability (HRV) and blood pressure can provide relevant information on autonomic nervous system (ANS) dynamics. For example, the high-frequency (HF) power of HRV series reflects the parasympathetic nervous control on heart rate, whereas the power in low-frequency (LF) band is influenced by both sympathetic and parasympathetic systems (12, 13). Several previous studies emphasized that the LF component of arterial blood pressure variability (BPV) can be understood as a marker of sympathetic modulation of peripheral vasculature (14–16). Concerning the correlation between ANS electrophysiological parameters and levels of plasma neurotransmitters, a decrease of LF power of blood pressure was associated with a reflex-mediated reduction in sympathetic nerve activity, demonstrated by lower plasma noradrenaline levels (17). Moreover, normalized values of LF power of HRV and its low/high-frequency ratio increased with plasma catecholamines, whereas normalized HF power decreased in response to head-up tilt or hypoglycemia (18). Although the investigation of brain activity during dreams has allowed researchers to identify specific areas and markers, the results related to autonomic correlates remain mostly limited to the discrimination of sleep stages. Autonomic balance during REM sleep was hypothesized to be similar to that during wakefulness, whereas a decrease in sympathetic activity was associated with NREM stage (19, 20). Similar long-range correlations were also identified in both REM stage and wakefulness by detrended fluctuation analysis of HRV series (21). A shift from vagal to sympathetic activity was highlighted during REM stages by studies investigating heart rate variability (HRV) dynamics (20, 22, 23) and blood pressure fluctuations (24, 25). Sleep-dependent changes in the coupling between HRV and blood pressure were investigated, and the highest values of the cross-correlation function between the fluctuations of heart periods and systolic blood pressure were found during deep NREM sleep (26). Investigation of autonomic responses related to dream periods during lucid dreaming in REM sleep highlighted increases in eye movement density, heart rate, and respiration rate during this stage (27). In specific dream-correlated pathologies such as nightmare disorder, a sympathetic drive (28) and an increased heartbeat-evoked potential (29) were reported during REM sleep.

Although significant changes in the brain and autonomic activities have been reported during sleep, their synchronized action and triggering effect during a dream recall is not clear yet. The activation-synthesis hypothesis proposed by Hobson and McCarley (30) indicates that mental activity associated with dreaming may be the attempt of the thalamocortical system to make sense of ascending stimuli, such as brainstem generated ponto-geniculo-occipital waves. Other studies described brain and autonomic dynamics during dream-related disorders; in the study by Simor et al. (31), authors highlighted that abnormal arousal processes, which are characterized by an increase of autonomic sympathetic and EEG wake-like α activities, were present in subjects affected by nightmare disorder. Although consistent results were found on both the brain and autonomic system, the synchronized and directional CNS-ANS coupling was not investigated.

Here, we perform a comprehensive study on synchronized CNS and ANS activities during REM sleep by analyzing EEG and HRV together with arterial blood pressure series to determine significant causal differences between subjects with and without dream recalls, when awakened from sleep. Our aim was to investigate not only the effects of dream experience on both CNS and ANS signals but also the directional relationship in the time-frequency domain between central and peripheral dynamics during REM sleep, shortly before dream recall-associated and nondream recall-associated awakenings. In this way, we uncover a timeline of physiological arousals to explain the trigger for a dream experience during REM sleep. Even if preliminary, this is the first study to conduct a causal, time-frequency analysis of CNS-ANS interaction, including those on arterial blood pressure, to investigate dream physiology. Ad hoc brain-heart interaction (BHI) estimation methods have been proposed in the past to investigate the specific functional and directional information exchange between CNS and ANS (32–34). However, to the best of our knowledge, directed BHI estimations have not been performed in dream-related studies.

MATERIALS AND METHODS

Experimental Protocol

In this study, we conducted polysomnography on nine subjects (age: 19–36 yr, 5 women) to monitor their physiological signals during dreaming periods. The study was approved by the Bioethics Committee of the University of Pisa (Approval Number 2-2020). Each participant gave a written informed consent before starting the experiment. We recorded EEG and electrocardiography (ECG) signals using a Micromed Brain Quick LTM Holter EEG system. We also monitored their arterial blood pressure dynamics by continuously recording their blood pressure signals using a Finapres/Portapres system (Finapres Medical Systems, Enschede, the Netherlands), an acquisition system that records continuous estimates of cardiac output from the peripheral pulse in digital arteries, alternating between two fingers throughout the night. The Finapres system is the most suitable option to measure diastolic and systolic blood pressure, with high-temporal resolution, in a continuous and noninvasive manner.

The subjects were left in a dark room and allowed to sleep through the night as we monitored their sleep patterns from an adjacent room. During every REM episode, particularly, 5 min after the beginning of each REM episode, the subjects were woken by an alarm and questioned through a speaker (the questionnaire used in the experiment is in the Supplemental Data; all Supplemental material is available at https://doi.org/10.5281/zenodo.5585336). The questions inquired about the content of their dreams (i.e., sensory content, whether the sensations were positive or negative, etc.). Subsequently, the subjects were allowed to go back to sleep

until their next REM episode. A questionnaire was then filled in one last time by the subject on their final awakening on the subsequent morning. The number of dream experience (DE) and no dream experience (NE) reports for each subject is shown in Table 1.

Signal Processing

All the signals were recorded with a sampling rate of 512 Hz. EEG and autonomic signals from one female subject were discarded because of low quality.

For each REM segment, the polysomnographic acquisition corresponding to the 5-min period before awakening the subject was divided into nonoverlapping windows of 30 s. In this way, for each 30-s window, we obtained one sample of each feature extracted from any signal acquired during the experimental protocol [EEG, HRV, systolic arterial pressure (SAP), or diastolic arterial pressure (DAP)]. The 30-s windows related to corrupted signals were discarded from successive analyses. Subsequently, two groups of signals were considered: 30-s windows that were followed by a dream recall upon awakening (dream experience, DE) and 30-s windows upon awakening that did not result in any dream recall (no dream experience, NE).

A further analysis was performed again using 30-s windows that were shifted by 5 s over time to cover all the 5 min of REM phase for each acquisition. In this way, a detailed time-variant analysis of the main parameters extracted from the central and autonomic nervous dynamics was carried out to observe the differences in activity over time in the two groups.

In *Processing of EEG signals*, we describe the method used for processing the EEG signal segments acquired during the last 5 min before awakening. The signal processing methods described in *Processing of ANS signals* have been applied to each window of HRV, SAP, and DAP signals.

Processing of EEG signals.

The processing of the EEG signal followed a standard pipeline (35): band-pass filtering, bad channel rejection, artifact removal after wavelet-enhanced independent component analysis (wICA), and data re-referencing to the common average (34). All the preprocessing steps were implemented using MATLAB software and EEGLAB toolbox.

More specifically, the first step involved derivation of the normed joint probability of average log power from 1 Hz to 70 Hz; thus, channels belonging to the external 1% distribution tails were marked as bad channels and rejected. Subsequently, EEG series below 0.5 Hz and above 50 Hz were band-pass filtered by using the multitaper regression (35), thus removing electrical main frequency and LF noise. The subsequent step involved the application of wICA decomposition, which is able to detect and reject muscular and ocular activities and discontinuities (35). A machine learning algorithm was also applied to recognize artifacts in wICA-derived components (35). To recover the rejected channels, a spherical interpolation algorithm, which exploits neighbor EEG data, was used. Eventually, the time-varying average from all channels was derived to re-reference the EEG series (i.e., average referencing).

Power spectral density (PSD) of each EEG channel was estimated using the well-known Welch method. Specifically, we used a Hamming window of 2,048 samples (4 s) overlapping for 75% (3 s) to achieve a good time resolution.

The obtained PSD was then filtered to obtain the time course of the power in the five standard frequency bands:

- δ band from 0.5 to 4 Hz,
- θ band from 4 to 8 Hz,
- α band from 8 to 12 Hz,
- β band from 12 to 30 Hz, and
- γ band from 30 to 50 Hz.

Moreover, in a previous study (11), a novel index was defined to discriminate the dreaming experience from the nondreaming one; we used this index in this study. It is defined as the HF/LF ratio, where HF is the PSD in the frequency range of [20–50] Hz, and LF is the PSD in the δ band. The HF/LF ratio could be derived as a time series by using the time course of both the PSDs involved.

Processing of ANS signals.

We used the automatic algorithm developed by Pan–Tompkins to automatically identify the RR series from the ECG (36). Artifacts and ectopic beats were corrected using Kubios HRV software. Blood pressure signals were preprocessed using a 0.05–40 Hz Butterworth-approximated band-pass filter. A shape-preserving piecewise cubic interpolation at the standard rate of 4 Hz was applied to all series.

By analyzing ANS time series, we computed the smoothed pseudo Wigner–Ville distribution (SPWVD) of data corresponding to the last 5 min before awakening (37). Subsequently, we divided each time-frequency spectrum into windows of 30 s and calculated the mean PSD within LF and HF bands. With regards to HRV analysis, we used the standard ranges, that is, from 0.04 to 0.15 Hz for the LF band and from 0.15 to 0.4 Hz for the HF band. The frequency ranges used for DAP and SAP were as follows: from 0.07 to 0.13 Hz for LF power analysis (Mayer wave-related) and from 0.13 to 0.4 Hz for HF power analysis (38, 39).

The following features were extracted from each HRV, SAP, and DAP:

- LF power n.u., the power in LF band in normalized units ($LF_{power}/LF_{power} + HF_{power}$);
- HF power n.u., the power in HF band in normalized units ($HF_{power}/LF_{power} + HF_{power}$); and
- LF/HF, the ratio between the power values in LF band and HF band.

Table 1. *Number of DE and NE reports reported by each subject after awakenings*

Subject ID	DE	NE
Subject 1	1	
Subject 2	1	1
Subject 3		1
Subject 4	3	2
Subject 5		1
Subject 6	2	1
Subject 7	3	
Subject 8	2	

DE, dream experience; NE, no dream experience.

Brain-heart interaction estimation.

We estimated functional directional BHI by exploiting the synthetic data generation (SDG) model proposed in a previous study (32). It consists of a mathematical model that assesses the bidirectional modulations between EEG oscillations in a given frequency band and heartbeat-derived series for either HF or LF bands. The formulation models the EEG power time series as an adaptive Markov process amplitude model and the heartbeat dynamics through an integral pulse frequency modulation model (32). The two mathematical models are then combined into a unified model, wherein the coupling coefficients quantify the functional BHI in different directions and different combinations of frequency bands from both signals. To quantify the interaction parameters, the least squares method and Poincaré plot features were used. A comprehensive mathematical formulation can be found in a previous report (32).

The SDG method provides the possibility of estimating real-time BHI changes using the time resolution of the power series as an input. The SDG method was tested under strong sympathovagal elicitation; it showed peculiar bidirectional BHI dynamics (32).

Statistical Analysis

For each REM segment, we divided the time series into nonoverlapped windows of 30 s. Consequently, 10 samples were obtained for each feature derived from ANS and EEG signals. A total of 130 windows of 30 s that were followed by a dream recall upon awakening (dream experience, DE) and 50 windows of 30 s upon awakening that did not result in any dream recall (no dream experience, NE) were considered. Data segments belonging to REM periods before each awakenings are considered as independent samples. To elucidate statistically significant differences between the DE and NE groups, we used the Mann–Whitney nonparametric statistical test, with a significance level fixed at 5%.

With regard to EEG, the values of power in each frequency band (i.e., δ, θ, α, β, and γ) were compared between the two groups (i.e., DE and NE). EEG electrodes found significant underwent a thorough statistical analysis, in which Mann–Whitney test was applied to each bin of 0.25 Hz, in a range between 0.5 and 50 Hz. Moreover, Mann–Whitney test on the 30-s windows estimated was performed to the HF/LF ratio. HF/LF ratios of the entire time course (i.e., before the windowing operation) were also compared between the DE and NE groups over time; we extracted the mean value of HF/LF ratios from 30-s windows with a 5-s time-shift.

All the *P* values extracted from EEG analysis were adjusted using a permutation test correction with 1,000 permutations. A further cluster-mass permutation test (40) was performed to calculate the minimum dimension of cluster to be considered as significant (with 0.05% of significance) that has been successively imposed (minimum cluster size found equal to 3).

With regard to the ANS signals, the values of frequency parameters (LF n.u., HF n.u., LF/HF) extracted from 30-s time windows of HRV, SAP, and DAP signals were subjected to Mann–Whitney statistical test. Subsequently, for each frequency parameter, we extracted mean values from 30-s windows with a 5-s time-shift. Therefore, we computed a statistical analysis over the 5 min of REM period, applying a Mann–Whitney statistical test between NE and DE groups every 5 s.

Regarding BHI estimates, statistical analyses similar to those performed to compare EEG and ANS estimates were performed. Specifically, we extracted mean values from 30-s windows with a 5-s time-shift. Therefore, we computed a statistical analysis over the 5-min REM period, applying a Mann–Whitney statistical test between NE and DE groups every 5 s. All the *P* values extracted from BHI analysis have been adjusted using a permutation test correction with 1,000 permutations.

In this study, the use of nonparametric tests is justified by the non-Gaussian distribution of samples, which was determined using Shapiro–Wilk test.

RESULTS

EEG Signal Analysis

There were significant differences between EEG power values of the dream experience (DE) and no dream experience (NE) groups. The results obtained in the conventional frequency bands (δ, θ, α, β, γ) were computed over the 5-min period preceding the awakening and are shown in Fig. 1.

During a dream experience, we observed a significant decrease in spectral power over the parieto-occipital areas encompassing the entire frequency spectrum. This region is larger in θ, α, and β bands than in δ and γ bands. This region is symmetric in high-frequency bands (i.e., β and γ bands) and more evident on the left hemisphere in LF bands (i.e., δ, θ, and α). Spectrum obtained by channel O1, which is located in the occipital region, is shown as example. Moreover, a significant increase of median EEG power, across all frequency bands, was detected by a cluster of electrodes belonging to the centrofrontal areas lateralized to the left prefrontal region. Channel F3 is one such cluster (Fig. 1).

Figure 2*A* shows the HF/LF values of the EEG series. The topographic images depict a broad centroparietal region highlighting a statistically significant difference between the DE and NE groups. As a general result, the ratio seems to be higher during the DE phase than during the NE phase.

ANS Signal Analysis

Concerning the statistical analysis of autonomic signals in the frequency domain, considering nonoverlapping 30-s windows, we found interesting differences between the groups NE and DE. Table 2 shows the P values obtained from Mann–Whitney statistical tests on LF power n.u., HF power n.u., and LF/HF values of HRV, SAP, and DAP time series. Results showed significant differences in HRV ($P < 0.01$) and SAP ($P < 0.05$) features between the two groups. Boxplots of HRV and SAP values in DE and NE groups are reported in Figs. 3 and 4, respectively. Median values of the normalized power in HF band were lower in the DE group than in the NE group. For both HRV and SAP signals, LF power n.u. and LF/HF values were significantly higher in the DE group than in NE group. Frequency analysis of DAP series did not reveal statistically significant differences between the DE and NE groups.

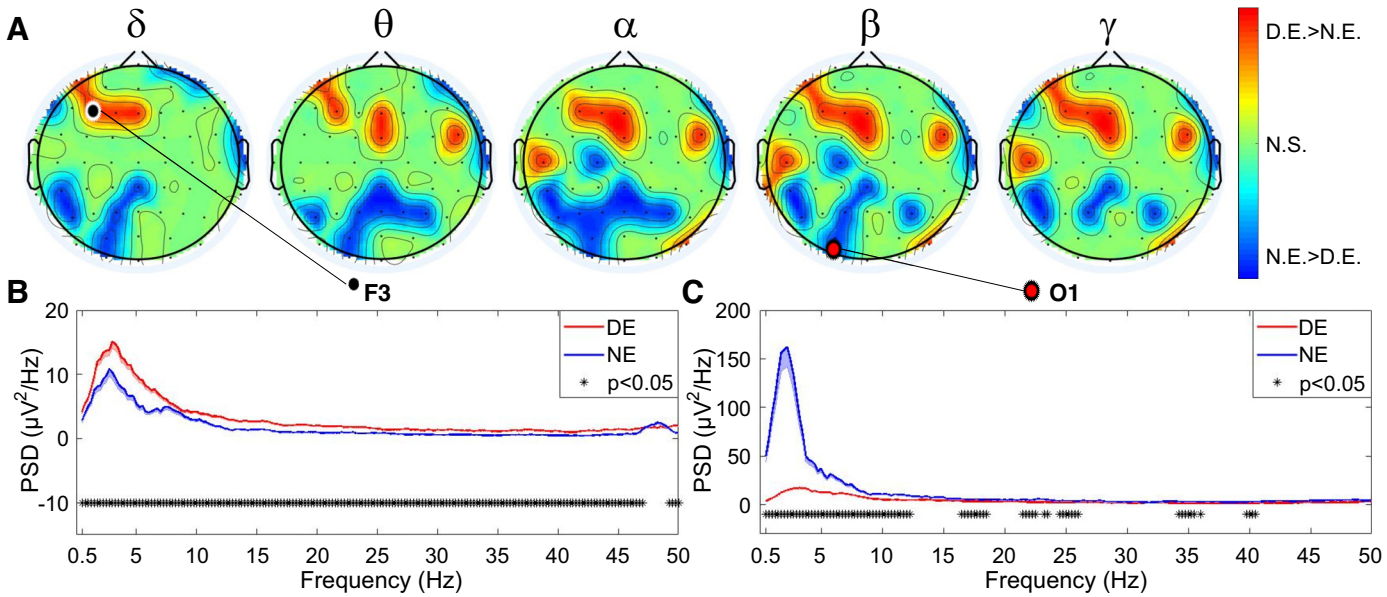

Figure 1. *A*: topographical representation of electroencephalography (EEG) power values of the dream experience (DE) and no dream experience (NE) groups corresponding to the 5 frequency bands (δ, θ, α, β, γ). Electrodes associated with insignificant *P* values are highlighted in green. Red spots indicate the cortical areas showing an increase in the median power in the DE group than in the NE group. Blue spots indicate the cortical areas showing a decrease in the median power in the DE group than in the NE group. Two examples of EEG median spectra related to channels F3 (*B*) and O1 (*C*) are also shown. Asterisks in *B* and *C* refer to statistically significant differences between the DE and NE groups (Mann–Whitney test). N.S., not significant; PSD, power spectral density.

Time-Varying Analysis and BHI Estimation

All traces appear homogeneous under the DE and NE conditions up to 265 s before the awakening (Fig. 2*B*). ANS parameters extracted from HRV, DAP, and SAP series were compared between the DE and NE groups using Mann–Whitney nonparametric test. With regard to LF power in normalized units (LF power n.u.) of DAP signals, the significant time window was centered in the range of [−265, −250] s (Fig. 2*B*). Mann–Whitney test showed that LF/HF_{DAP} values were significantly higher in the DE group than in the NE group within the same time window. The HF power in normalized units (HF power n.u.) values within the same time window were different between the two groups; however, in this case, the values were higher in the NE group than in the DE group.

SAP frequency parameters showed similar trends. However, no statistically significant differences were found.

Regarding the EEG signals, the time course of the HF/LF ratio corresponding to channel C2 is presented in Fig. 2*B*. The reported channel was selected among those found significant in Fig. 2*A*. A significant and clear difference between the two experimental conditions can be noted in the time windows [−175, −155] and [−100, −90] before awakening from REM sleep.

Analysis of the temporal dynamics of HRV frequency parameters revealed a significant difference centered in the [−130, −115] s window preceding the awakening, with higher values observed in the DE group than in the NE group (Fig. 2*B*). Median values of LF power $n.u._{HRV}$ were higher in the DE group than in the NE group, whereas those of HF power $n.u._{HRV}$ were lower in the DE group than in the NE group.

Figure 2*B* shows the BHI estimated using the SDG method, particularly in the heart-to-brain direction, involving the HF and γ bands, for HRV and EEG (channel C2), respectively. After approximately 120 s, the DE group showed a greater increase in HF-to-γ interplay than did the NE group, and this trend is maintained until few seconds before the awakening. Mann–Whitney test revealed a significant difference between the groups in a 40-s time window (i.e., between −135 s and −95 s before the awakening).

DISCUSSION

In this study, we conducted a comprehensive analysis of dream-related CNS-ANS physiological patterns with a particular focus on the differences between awakenings with and without memories of dreams (DE vs. NE). We investigated central and autonomic dynamics during REM periods using continuous arterial blood pressure signals acquired from nine healthy subjects simultaneously during polysomnography monitoring using a 64-channel EEG system. Furthermore, we estimated functional BHI using an ad hoc computational model. The aim of the study was to uncover a causal brain-body network associated with dream reports. Accordingly, we studied brain and cardiovascular signals both separately and through advanced methods for a functional BHI estimation. An overall timeline of CNS and ANS activation was also proposed. The experimental protocol was designed to divide the acquisitions into two groups, as described previously (11): one group involved recall of a dream experience after awakening (DE) and the other group did not involve dream recall (NE). The aim of the study was to identify differences in physiological parameters extracted from CNS signals (i.e., EEG), ANS signals (i.e., HRV, SAP, and DAP), and their directed functional interaction between the two groups.

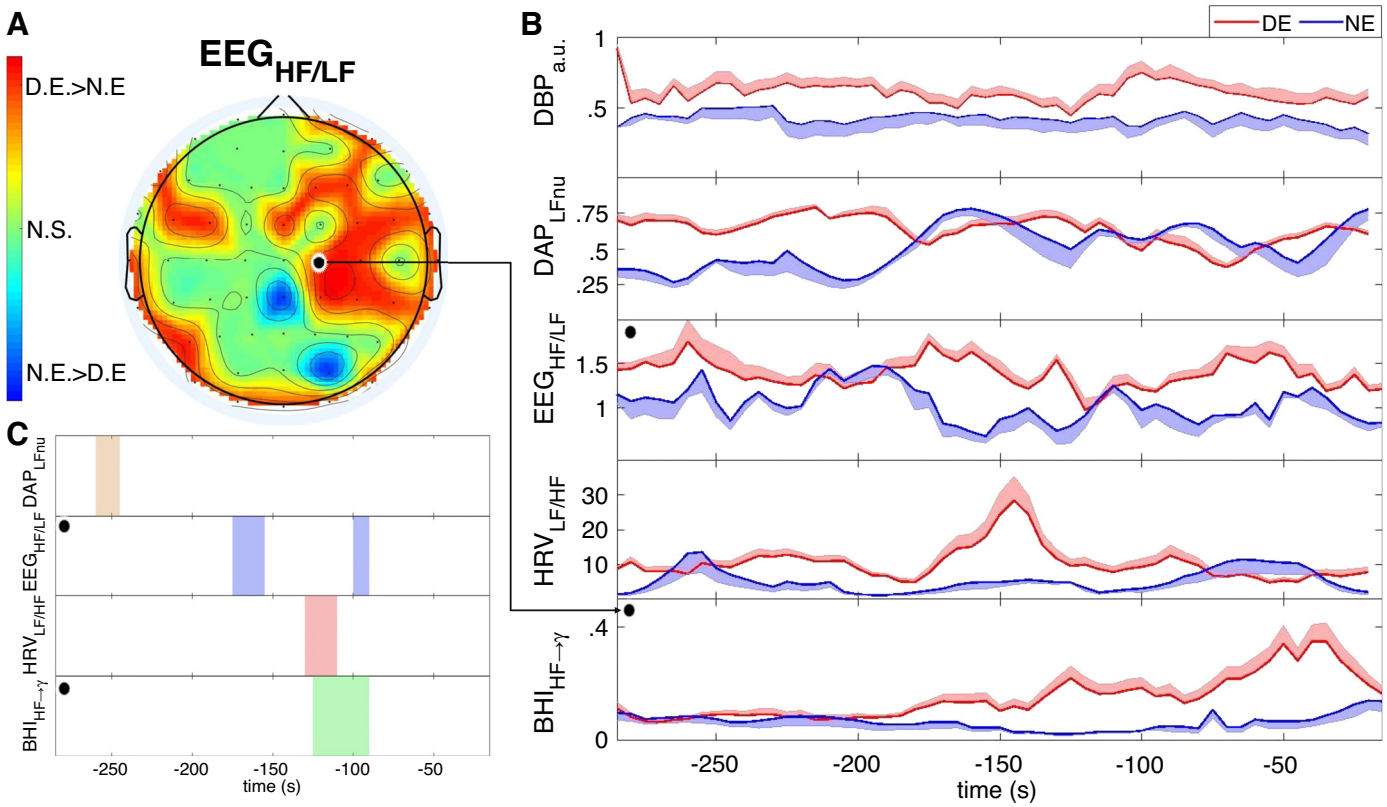

Figure 2. *A*: topographical representation of Mann–Whitney statistical analysis on the low-frequency/high-frequency (HF/LF) power ratios of the dream experience (DE) and no dream experience (NE) groups. Red spots indicate the cortical areas showing an increase in the median power in the DE group than in the NE group, and blue spots represent the opposite. *B*: median and median absolute deviation (MAD) values for the following features (from *top* to *bottom*) were determined by time series analysis of data acquired in the 5 min before awakening: mean diastolic blood pressure (DBP), LF in normalized units (LF n.u.) of diastolic arterial pressure (DAP) series, HF/LF ratio of the electroencephalography (EEG) signal acquired from channel C2, LF/HF ratio of heart rate variability (HRV) series, and brain-heart interaction (BHI) estimated using the synthetic data generation (SDG) method in the direction from the heart to the brain, i.e., from HRV-HF oscillations to the EEG-γ oscillations from C2 electrode. Red- and blue-colored trend lines represent the DE and NE groups, respectively; the *P* values have been adjusted for multiple comparisons using permutation test. *C*: statistically significant differences between the DE and NE groups along the time for the 4 features are shown in *B*. a.u., arbitrary unit; N.S., not significant.

Regarding EEG signal analysis, Mann–Whitney nonparametric test was used to compare power spectral density (PSD) values of the EEG signals related to the DE and NE group, considering each 0.25-Hz frequency bin within the range of 0.5–50 Hz. A permutation test was used to adjust the significance threshold. In this study, we found that 41 EEG channels presented significant differences in the EEG power values between the two groups. Our results corroborate those reported by Siclari et al. (11) that observed a decrease in LF activity associated with dream experience in the parieto-occipital region and an increase in high-frequency power ($f > 20$ Hz) in the frontal areas (Fig. 1). In the study by Siclari et al. (11), a "hot posterior zone," which refers to an increase in the activity in the central and posterior right hemisphere, was reported; similar findings were observed in the current study. This can be observed in Fig. 2*A*, wherein the results corresponding to the coefficient HF/LF—which was proposed in the study by Siclari et al. (11)—are presented. Previous studies suggested the lateralization of EEG activity to the right hemisphere, which is more involved in visuospatial functioning (41), during dreaming experience. More specifically, the right hemisphere has been found to be activated during nonconscious emotional perception (42).

This activation in the right hemisphere in the DE group was also reported in γ band. The relationship between γ-band activity and emotions has already been investigated in a previous study and an increase in activity was found to be associated with emotionally and socially relevant stimuli,

Table 2. *Results from a Mann–Whitney statistical test applied to LF power n.u., HF power n.u., and LF/HF computed from the HRV, SAP, and DAP signals to discern DE and NE groups*

	Mann–Whitney *P* Values		
	HRV	SAP	DAP
LF power n.u.	**0.0049**	**0.0304**	0.1172
HF power n.u.	**0.0049**	**0.0304**	0.1172
LF/HF	**0.0049**	**0.0304**	0.1172

Bold characters indicate significant $P < 0.05$. DAP, diastolic arterial pressure; DE, dream experience; HF, high frequency; HRV, heart rate variability; LF, low frequency; NE, no dream experience; n.u., normalized unit; SAP, systolic arterial pressure.

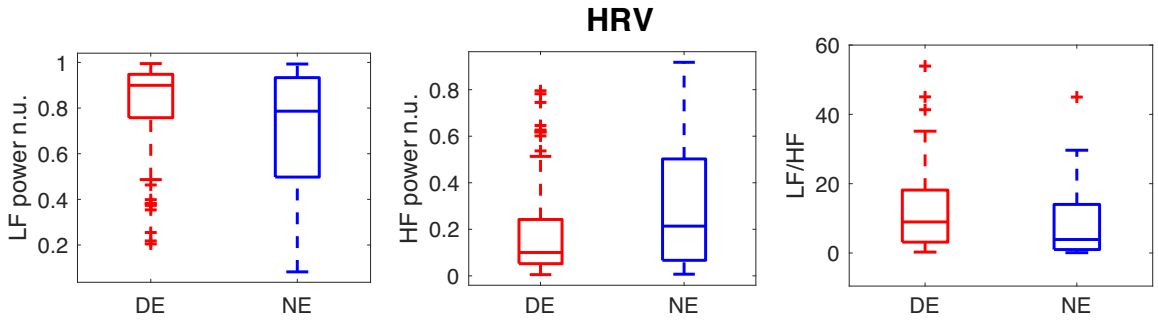

Figure 3. Box-plots of heart rate variability (HRV) features defined in the frequency domain that resulted significantly different in the comparison between the two groups ($P < 0.05$). Red color indicates the dream experience (DE) group, and blue color indicates the no dream experience (NE) group. HF, high frequency; LF, low frequency; n.u., normalized unit.

for example, response to negative facial expressions (43) and familiar versus unfamiliar faces (44).

Regarding the processing of autonomic signals, HRV series was extracted from ECG, whereas the series constituted by the amplitudes of systolic and diastolic peaks, that is, SAP and DAP, were extracted from arterial blood pressure signals. The parameters extracted from HRV and SAP series using frequency domain features showed statistically significant differences between the two groups (Table 1 and Figs. 1 and 2). An overall increase in sympathetic activity in association with dream experience recall was observed, as indicated by an increase in LF power n.u. and LF/HF values in both HRV and SAP series analyses. A parallel decrease in vagal activity can be deduced from a significant decrease in HF power n.u. and HF power.

The increase in sympathetic activity is a conventional response to arousing stimuli, as anger- or fear/anxiety-inducing situations (45). In our previous studies, we demonstrated the efficiency of ANS signals as markers of moods and emotions (46–50). It can be hypothesized, at a speculative level, that these findings can be related to emotion arousal during dreams. In the study by Merritt et al. (51), for example, the 95% of dream reports was associated with a specific emotional content, and anxiety was identified in the 32% of dream recalls.

Consistently with the hypotheses, we found statistically significant results from time-varying analysis of frequency parameters extracted from CNS and ANS series. As shown in Fig. 2, dynamics of the three examined systems, that is, CNS, cardiac system, and vascular system, differ significantly between the two groups in discernible time windows. Specifically, we found a significant early variation in the low-frequency components of diastolic pressure (LFn.u.$_{DAP}$), 265 s before the awakening from the REM phase. This variation can be attributed to an independent peripheral phenomenon, possibly because of thermal oscillations or fluctuations of hormonal concentrations (30). Subsequently, with regard to EEG signals, a significant difference was found in the median trend of HF/LF of the C2 channel ~3 min before awakening ([−175, −155] s before the awakening). The succession of these two significant changes in activity over time, where the first is peripheral and the second is related to the CNS, supports the hypotheses presented by Hobson and McCarley (30). According to their ascending activation theory, dreaming experience is a function of sensory motor information that arises from peripheral signals and is then relayed from the brain stem to the cerebral cortex. However, in our findings, a relevant change in HRV dynamics follows the first variations in the EEG. Therefore, it can be hypothesized that after activation at the brain level attributable to dream experience, a top-down interaction causes a canonical autonomic activation found in the significant variation of LF/HF ratio in the HRV. More specifically, results from the heart-to-brain interaction analysis suggest that the interactions between CNS and ANS associated with dreaming experience are bidirectional and exhibit dynamic changes. As a matter of fact, in the same scalp region that showed enhanced EEG signals (i.e., C2 electrode), BHI$_{HF\rightarrow\gamma}$

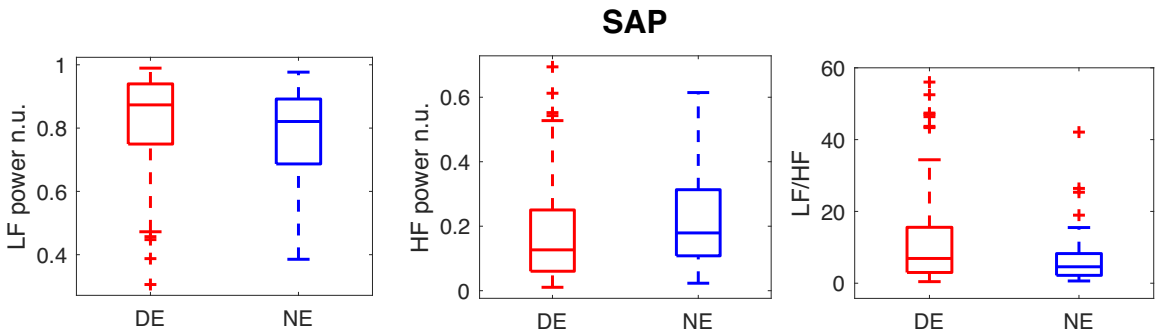

Figure 4. Box-plots of systolic arterial pressure (SAP) features defined in the frequency domain that resulted to be significant in the comparison between the two groups ($P < 0.05$). Red color indicates the dream experience (DE) group, and blue color indicates the no dream experience (NE) group. HF, high frequency; LF, low frequency; n.u., normalized unit.

depicts a clear increasing trend in the DE group, whereas in the NE one a constant behavior is shown. The difference is statistically significant in a time window defined by 135 s to 95 s before the awakening. Notably, such a time window comes after the significant period depicted by ANS-LF/HF ratio and before the second significant time window from the EEG-HF/LF analysis, thus enhancing a persistent peripheral action over the brain dynamics during dreaming experience. However, it cannot be excluded that our data also fit other hypotheses concerning the information flow between CNS and ANS sleep mentation (52, 53).

The major limitation of this preliminary study is the reduced number of data samples from independent subjects. This limitation led us to consider data segments preceding each awakening with or without recall of dreams as independent samples. With the appropriate statistical power, paired statistics could be properly applied also to discern physiological dynamics based on the sex and emotional content of dreams. Therefore, future endeavors will be directed at increasing the number of subjects, also investigating a within-subject normalization and comparing the effect of dreams in CNS-ANS dynamics in REM and NREM stages through a paired analysis. Furthermore, it is necessary to investigate the valence of such physiological axis in modulating dream experience.

SUPPLEMENTAL DATA

Supplemental Data: https://doi.org/10.5281/zenodo.5585336.

DISCLOSURES

No conflicts of interest, financial or otherwise, are declared by the authors.

AUTHOR CONTRIBUTIONS

R.M.B., U.F., and G.V. conceived and designed research; G.G. and T.B. performed experiments; M.N. and V.C. analyzed data; M.N., V.C., R.M.B., E.P.S., U.F., and G.V. interpreted results of experiments; M.N. and V.C. prepared figures; M.N. drafted manuscript; M.N., R.M.B., E.P.S., U.F., and G.V. edited and revised manuscript; M.N., V.C., G.G., T.B., R.M.B., E.P.S., U.F., and G.V. approved final version of manuscript.

REFERENCES

1. **de Zambotti M**, **Trinder J**, **Silvani A**, **Colrain IM**, **Baker FC.** Dynamic coupling between the central and autonomic nervous systems during sleep: a review. *Neurosci Biobehav Rev* 90: 84–103, 2018. doi:10.1016/j.neubiorev.2018.03.027.
2. **Silvani A**, **Dampney RA.** Central control of cardiovascular function during sleep. *Am J Physiol Heart Circ Physiol* 305: H1683–H1692, 2013. doi:10.1152/ajpheart.00554.2013.
3. **Scammell TE**, **Arrigoni E**, **Lipton JO.** Neural circuitry of wakefulness and sleep. *Neuron* 93: 747–765, 2017. doi:10.1016/j.neuron.2017.01.014.
4. **Siclari F**, **Valli K**, **Arnulf I.** Dreams and nightmares in healthy adults and in patients with sleep and neurological disorders. *Lancet Neurol* 19: 849–859, 2020. doi:10.1016/S1474-4422(20)30275-1.
5. **Fosse R**, **Stickgold R**, **Hobson JA.** Brain-mind states: reciprocal variation in thoughts and hallucinations. *Psychol Sci* 12: 30–36, 2001. doi:10.1111/1467-9280.00306.
6. **Stickgold R**, **Malia A**, **Fosse R**, **Propper R**, **Hobson JA.** Brain-mind states: I. longitudinal field study of sleep/wake factors influencing mentation report length. *Sleep* 24: 171–179, 2001 [Erratum in *Sleep* 24: preceding table of contents, 2001]. doi:10.1093/sleep/24.2.171.
7. **Aserinsky E**, **Kleitman N.** Regularly occurring periods of eye motility, and concomitant phenomena, during sleep. *Science* 118: 273–274, 1953.doi:10.1126/science.118.3062.273.
8. **Dement W**, **Kleitman N.** The relation of eye movements during sleep to dream activity: an objective method for the study of dreaming. *J Exp Psychol* 53: 339–346, 1957. doi:10.1037/h0048189.
9. **Dement W**, **Kleitman N.** Cyclic variations in EEG during sleep and their relation to eye movements, body motility, and dreaming. *Electroencephalogr Clin Neurophysiol* 9: 673–690, 1957.doi:10.1016/0013-4694(57)90088-3.
10. **Llinás R**, **Ribary U.** Coherent 40-hz oscillation characterizes dream state in humans. *Proc Natl Acad Sci USA* 90: 2078–2081, 1993. doi:10.1073/pnas.90.5.2078.
11. **Siclari F**, **Baird B**, **Perogamvros L**, **Bernardi G**, **LaRocque JJ**, **Riedner B**, **Boly M**, **Postle BR**, **Tononi G.** The neural correlates of dreaming. *Nat Neurosci* 20: 872–878, 2017. doi:10.1038/nn.4545.
12. **Valenza G**, **Citi L**, **Saul JP**, **Barbieri R.** Measures of sympathetic and parasympathetic autonomic outflow from heartbeat dynamics. *J Appl Physiol (1985)* 125: 19–39, 2018. doi:10.1152/japplphysiol.00842.2017.
13. **Reyes del Paso GA**, **Langewitz W**, **Mulder LJ**, **Van Roon A**, **Duschek S.** The utility of low frequency heart rate variability as an index of sympathetic cardiac tone: a review with emphasis on a reanalysis of previous studies. *Psychophysiology* 50: 477–487, 2013. doi:10.1111/psyp.12027.
14. **Pagani M**, **Montano N**, **Porta A**, **Malliani A**, **Abboud FM**, **Birkett C**, **Somers VK.** Relationship between spectral components of cardiovascular variabilities and direct measures of muscle sympathetic nerve activity in humans. *Circulation* 95: 1441–1448, 1997. doi:10.1161/01.CIR.95.6.1441.
15. **El Sayed K**, **Macefield VG**, **Hissen SL**, **Joyner MJ**, **Taylor CE.** Rate of rise in diastolic blood pressure influences vascular sympathetic response to mental stress. *J Physiol* 594: 7465–7482, 2016. doi:10.1113/JP272963.
16. **Barbic F**, **Heusser K**, **Marchi A**, **Zamunér AR**, **Gauger P**, **Tank J**, **Jordan J**, **Diedrich A**, **Robertson D**, **Dipaola F**, **Achenza S**, **Porta A**, **Furlan R.** Cardiovascular parameters and neural sympathetic discharge variability before orthostatic syncope: role of sympathetic baroreflex control to the vessels. *Physiol Meas* 36: 633–641, 2015. doi:10.1088/0967-3334/36/4/633.
17. **Castellano M**, **Rizzoni D**, **Beschi M**, **Muiesan ML**, **Porteri E**, **Bettoni G**, **Salvetti M**, **Cinelli A**, **Zulli R**, **Agabiti-Rosei E.** Relationship between sympathetic nervous system activity, baroreflex and cardiovascular effects after acute nitric oxide synthesis inhibition in humans. *J Hypertens* 13: 1153–1161, 1995. doi:10.1097/00004872-199510000-00010.
18. **Vlcek M**, **Radikova Z**, **Penesova A**, **Kvetnansky R**, **Imrich R.** Heart rate variability and catecholamines during hypoglycemia and orthostasis. *Auton Neurosci* 143: 53–57, 2008. doi:10.1016/j.autneu.2008.08.001.
19. **Trinder J**, **Kleiman J**, **Carrington M**, **Smith S**, **Breen S**, **Tan N**, **Kim Y.** Autonomic activity during human sleep as a function of time and sleep stage. *J Sleep Res* 10: 253–264, 2001. doi:10.1046/j.1365-2869.2001.00263.x.
20. **Chouchou F**, **Desseilles M.** Heart rate variability: a tool to explore the sleeping brain? *Front Neurosci* 8: 402, 2014. doi:10.3389/fnins.2014.00402.
21. **Bunde A**, **Havlin S**, **Kantelhardt JW**, **Penzel T**, **Peter J-H**, **Voigt K.** Correlated and uncorrelated regions in heart-rate fluctuations during sleep. *Phys Rev Lett* 85: 3736–3739, 2000. doi:10.1103/PhysRevLett.85.3736.
22. **Cabiddu R**, **Cerutti S**, **Viardot G**, **Werner S**, **Bianchi AM.** Modulation of the sympatho-vagal balance during sleep: frequency domain study of heart rate variability and respiration. *Front Physiol* 3: 45, 2012. doi:10.3389/fphys.2012.00045.
23. **Van De Borne P**, **Nguyen H**, **Biston P**, **Linkowski P**, **Degaute JP.** Effects of wake and sleep stages on the 24-h autonomic control of blood pressure and heart rate in recumbent men. *Am J Physiol Heart Circ Physiol* 266: H548–H554, 1994. doi:10.1152/ajpheart.1994.266.2.H548.

24. **Snyder F**, **Hobson JA**, **Morrison DF**, **Goldfrank F.** Changes in respiration, heart rate, and systolic blood pressure in human sleep. *J Appl Physiol* 19: 417–422, 1964. doi:10.1152/jappl.1964.19.3.417.
25. **Somers VK**, **Dyken ME**, **Mark AL**, **Abboud FM.** Sympathetic-nerve activity during sleep in normal subjects. *N Engl J Med* 328: 303–307, 1993. doi:10.1056/NEJM199302043280502.
26. **Silvani A**, **Grimaldi D**, **Vandi S**, **Barletta G**, **Vetrugno R**, **Provini F**, **Pierangeli G**, **Berteotti C**, **Montagna P**, **Zoccoli G**, **Cortelli P.** Sleep-dependent changes in the coupling between heart period and blood pressure in human subjects. *Am J Physiol Regul Integr Comp Physiol* 294: R1686–R1692, 2008. doi:10.1152/ajpregu.00756.2007.
27. **Brylowski A**, **Levitan L**, **LaBerge S.** H-reflex suppression and autonomic activation during lucid REM sleep: a case study. *Sleep* 12: 374–378, 1989. doi:10.1093/sleep/12.4.374.
28. **Nielsen T**, **Paquette T**, **Solomonova E**, **Lara-Carrasco J**, **Colombo R**, **Lanfranchi P.** Changes in cardiac variability after REM sleep deprivation in recurrent nightmares. *Sleep* 33: 113–122, 2010. doi:10.1093/sleep/33.1.113.
29. **Perogamvros L**, **Park H-D**, **Bayer L**, **Perrault AA**, **Blanke O**, **Schwartz S.** Increased heartbeat-evoked potential during REM sleep in nightmare disorder. *NeuroImage Clin* 22: 101701, 2019. doi:10.1016/j.nicl.2019.101701.
30. **Hobson JA**, **McCarley RW.** The brain as a dream state generator: an activation-synthesis hypothesis of the dream process. *Am J Psychiatry* 134: 1335–1348, 1977. doi:10.1176/ajp.134.12.1335.
31. **Simor P**, **Körmendi J**, **Horváth K**, **Gombos F**, **Ujma PP**, **Bódizs R.** Electroencephalographic and autonomic alterations in subjects with frequent nightmares during pre-and post-REM periods. *Brain Cogn* 91: 62–70, 2014. doi:10.1016/j.bandc.2014.08.004.
32. **Catrambone V**, **Greco A**, **Vanello N**, **Scilingo EP**, **Valenza G.** Time-resolved directional brain–heart interplay measurement through synthetic data generation models. *Ann Biomed Eng* 47: 1479–1489, 2019. doi:10.1007/s10439-019-02251-y.
33. **Catrambone V**, **Talebi A**, **Barbieri R**, **Valenza G.** Time-resolved brain-to-heart probabilistic information transfer estimation using inhomogeneous point-process models. *IEEE Trans Biomed Eng* 68: 3366–3374, 2021. doi:10.1109/TBME.2021.3071348.
34. **Candia-Rivera D**, **Catrambone V**, **Valenza G.** The role of electroencephalography electrical reference in the assessment of functional brain–heart interplay: from methodology to user guidelines. *J Neurosci Methods* 360: 109269, 2021.doi:10.1016/j.jneumeth.2021.109269.
35. **Gabard-Durnam LJ**, **Mendez Leal AS**, **Wilkinson CL**, **Levin AR.** The harvard automated processing pipeline for electroencephalography (HAPPE): standardized processing software for developmental and high-artifact data. *Front Neurosci* 12: 97, 2018. doi:10.3389/fnins.2018.00097.
36. **Pan J**, **Tompkins WJ.** A real-time QRS detection algorithm. *IEEE Trans Biomed Eng* 32: 230–236, 1985. doi:10.1109/TBME.1985.325532.
37. **Orini M**, **Bailón R**, **Mainardi LT**, **Laguna P**, **Flandrin P.** Characterization of dynamic interactions between cardiovascular signals by time-frequency coherence. *IEEE Trans Biomed Eng* 59: 663–673, 2012. doi:10.1109/TBME.2011.2171959.
38. **van Beek AH**, **Lagro J**, **Olde-Rikkert MG**, **Zhang R**, **Claassen JA.** Oscillations in cerebral blood flow and cortical oxygenation in Alzheimer's disease. *Neurobiol Aging* 33: 428.e21–428.e31, 2012. doi:10.1016/j.neurobiolaging.2010.11.016.
39. **Tayama J**, **Munakata M**, **Yoshinaga K**, **Toyota T.** Higher plasma homocysteine concentration is associated with more advanced systemic arterial stiffness and greater blood pressure response to stress in hypertensive patients. *Hypertens Res* 29: 403–409, 2006. doi:10.1291/hypres.29.403.
40. **Friston KJ**, **Worsley KJ**, **Frackowiak RS**, **Mazziotta JC**, **Evans AC.** Assessing the significance of focal activations using their spatial extent. *Hum Brain Mapp* 1: 210–220, 1994. doi:10.1002/hbm.460010306.
41. **Kerr NH**, **Foulkes D.** Right hemispheric mediation of dream visualization: a case study. *Cortex* 17: 603–609, 1981. doi:10.1016/S0010-9452(81)80066-4.
42. **Killgore WD**, **Yurgelun-Todd DA.** The right-hemisphere and valence hypotheses: could they both be right (and sometimes left)? *Soc Cogn Affect Neurosci* 2: 240–250, 2007. doi:10.1093/scan/nsm020.
43. **Schneider TR**, **Hipp JF**, **Domnick C**, **Carl C**, **Büchel C**, **Engel AK.** Modulation of neuronal oscillatory activity in the beta- and gamma-band is associated with current individual anxiety levels. *NeuroImage* 178: 423–434, 2018. doi:10.1016/j.neuroimage.2018.05.059.
44. **Anaki D**, **Zion-Golumbic E**, **Bentin S.** Electrophysiological neural mechanisms for detection, configural analysis and recognition of faces. *Neuroimage* 37: 1407–1416, 2007. doi:10.1016/j.neuroimage.2007.05.054.
45. **Kreibig SD.** Autonomic nervous system activity in emotion: a review. *Biol Psychol* 84: 394–421, 2010. doi:10.1016/j.biopsycho.2010.03.010.
46. **Nardelli M**, **Lanata A**, **Bertschy G**, **Scilingo EP**, **Valenza G.** Heartbeat complexity modulation in bipolar disorder during daytime and nighttime. *Sci Rep* 7: 17920, 2017. doi:10.1038/s41598-017-18036-z.
47. **Nardelli M**, **Greco A**, **Bolea J**, **Valenza G**, **Scilingo EP**, **Bailon R.** Reliability of lagged poincaré plot parameters in ultrashort heart rate variability series: application on affective sounds. *IEEE J Biomed Health Inform* 22: 741–749, 2018. doi:10.1109/JBHI.2017.2694999.
48. **Nardelli M**, **Greco A**, **Danzi OP**, **Perlini C**, **Tedeschi F**, **Scilingo EP**, **Del Piccolo L**, **Valenza G.** Cardiovascular assessment of supportive doctor-patient communication using multi-scale and multi-lag analysis of heartbeat dynamics. *Med Biol Eng Comput* 57: 123–134, 2019. doi:10.1007/s11517-018-1869-1.
49. **Greco A**, **Faes L**, **Catrambone V**, **Barbieri R**, **Scilingo EP**, **Valenza G.** Lateralization of directional brain-heart information transfer during visual emotional elicitation. *Am J Physiol Regul Integr Comp Physiol* 317: R25–R38, 2019. doi:10.1152/ajpregu.00151.2018.
50. **Catrambone V**, **Messerotti Benvenuti S**, **Gentili C**, **Valenza G.** Intensification of functional neural control on heartbeat dynamics in subclinical depression. *Transl Psychiatry* 11: 221, 2021. doi:10.1038/s41398-021-01336-4.
51. **Merritt JM**, **Stickgold R**, **Pace-Schott E**, **Williams J**, **Hobson JA.** Emotion profiles in the dreams of men and women. *Consciousness Cogn* 3: 46–60, 1994. doi:10.1006/ccog.1994.1004.
52. **Nielsen TA.** Chronobiological features of dream production. *Sleep Med Rev* 8: 403–424, 2004. doi:10.1016/j.smrv.2004.06.005.
53. **Nir Y**, **Tononi G.** Dreaming and the brain: from phenomenology to neurophysiology. *Trends Cogn Sci* 14: 88–100, 2010. doi:10.1016/j.tics.2009.12.001.